Zagazig University Medical Journal
www.zumj.journals.ekb.eg
https://doi.org/10.21608/zumj.2022.172531.2673 Volume 30, Issue 1, January 2024

Manuscript ID ZUMJ-2211-2673 (R1)
DOI 10.21608/ZUMJ.2022.172531.2673

ORIGINAL ARTICLE

Role of Adipose-Derived Stem Cells in Restoration of Histological Structure of Rat Frontal Cortex after Chronic Aspartame Intake.

Amani A. Almallah, Rania A. Galhom, Eman Mohammed Kamel*
Department of Human Anatomy & Embryology, Faculty of Medicine, Suez Canal University, Ismailia, Egypt

***Corresponding author**:

Eman Mohammed Kamel : lecturer of Human Anatomy &Embryology department, Faculty of Medicine, Suez Canal University, Ismailia, Egypt.

E-mail address:
Eman.M.Kamel@med.suez.edu.eg

Submit Date 2022-11-04
Revise Date 2022-12-15
Accept Date 2022-12-18

ABSTRACT

Background: Many reports on the use of aspartame revealed that it releases metabolites which in turn cause brain adverse effect on rats. Our aim was to investigate the impact of aspartame on histopathology and ultrastructure of rat frontal cortex and assess the efficacy of Adipose-Mesenchymal Stem Cells (AD-MSCs) to ameliorate this effect after chronic aspartame administration (40 mg/kg per body weight). **Methods:** to investigate the effects of aspartame, methotrexate and folate deficient diet was used to induce folate deficiency in rats to imitate the human methanol metabolic process. The animals were distributed into four groups; control group, MTX control, MXT/Aspartame and MXT/aspartame/AD-MSCs group. The histopathology and ultrastructure of frontal cortex along with its cell's expression of Caspase-3 and GFAP were assessed. The used AD-MSCs were characterized by immunohistochemical detection of CD73, CD105 and CD45 markers and tracked in frontal cortex by PCR. **Results:** White matter density was significantly reduced in MTX/aspartame animals, evidence of gliosis, pyramidal cell intracellular and extracellular vacuolations and Significant increase in Caspase-3 and GFAP stained neuron. Disorganization of ultrastructure organelles and oedematous astrocyte plates around blood vessels were evident when compared to control animals. Almost restoration of the frontal cortex architecture and ultrastructure was established in the MXT//aspartame/AD-MSCs together with significant decrease in Caspase-3 and GFAP stained neuron compared to MXT//aspartame group. **Conclusions:** AD-MSCs transplantation could mitigate the degenerative impact of aspartame metabolites on the rat frontal cortex.

Key words: Caspase 3; Adipose stem cell; Microscope Aspartame; Rat Frontal Cortex; GFAP

INTRODUCTION

Aspartame (L-aspartyl-L-phenylalanine methyl ester) is a common sweetener found in over 6,000 products, including carbonated soft drinks (Soda & juice), snacks, vitamins, and sugar-free cough syrups. [1]. It is used as a non-caloric source of sweetness in diabetics, as well as in weight loss and/or control regimens in place of sugar [2]. The acceptable daily consumption of aspartame, according to the European Food Safety Authority, is 40 mg / kg body weight per day [3].Aspartame is a white, crystalline, odorless powder that is converted in the intestinal lumen to phenylalanine (50 %), aspartic acid (40 %) & methanol (10 %) [2].

Aspartic acid is an excitatory organic molecule normally present in high concentrations in the brain, and its concentration is regulated by the blood brain barrier (BBB), which safeguards the brain against large fluctuations in plasma aspartate [4]. Phenylalanine is found in almost all protein-containing foods that is required for the formation of monoamines in the brain. Aspartame use may cause brain injury because of high phenylalanine levels in the blood.

Certain amino acids increase in the brain following aspartame intake. Methanol is another aspartame metabolite that is produced during aspartame digestion and has been linked to systemic toxicity. Aspartame and each of its metabolites have been researched in both humans and other animals at high doses. Each metabolite could have excite-toxic effects in animal model systems [4].

Phenylalanine, as a precursor of dopamine and norepinephrine, can influence brain levels of those neurotransmitters and thus brain functions. It can also influence serotonin biosynthesis in the brain by decreasing the uptake of tryptophan, a precursor of serotonin [5, 6]. It was also confirmed that methanol and its metabolites are neurotoxic, it is first transformed into formaldehyde and then formate. Therefore, superoxide anion and hydrogen peroxide are formed, mitochondrial damage subsequently occurs along with the release of oxygen radicals. Because of its high oxygen consumption, the brain is especially vulnerable to oxidative stress when compared to other organs; overproduction of free radicals causes the death of immature cortical neurons in culture and causes DNA damage. [4, 7, 8]. It has also been reported that the oxidative stress causes various neurodegenerative disorders by causing lipid peroxidation in the cell membrane [6]. As folate deficiency in rats is necessary to accumulate formate to develop metabolic acidosis, which is a feature of methanol poisoning, testing its toxicity is required. As rodents have high levels of liver folate content in their body so they couldn't develop acidosis and to mimic humans in the current study rat model, Methotrexate (MTX) consumption and a folate-deficient diet resulted in folate deficiency [6].

Numerous studies on short- and long-term aspartame consumption have revealed that excessive aspartame consumption may contribute to the pathogenesis of certain neurological and psychiatric disorders [5, 6]. However, there is a lack of studies, which focus on how to reduce or reverse the adverse degenerative effects of aspartame on brain tissue. Due to the fact that an innovative source for cytotherapy and regenerative medicine is mesenchymal stem cells (MSCs), we investigate in this study the possible ameliorative effects of adipose-derived mesenchymal stem cells (AD-MSCs) in aspartame-induced brain injury in albino rats. The transplantation of these cells has been extensively evaluated in numerous experimental and clinical trials for cardiovascular, immunological, and neurological disorders, with positive results. [9].

METHODS

Animals:

In addition to forty female Wistar albino rats weighing an average of 200-230 g, ten male Wistar albino rats served as donors of AD-MSCs for the experiments. All animal work were conducted in accordance with the National Institutes of Health's recommendations for the care and use of laboratory animals (NIH Publications No. 8023, revised 1978). Animals were kept in a conventional laboratory environment with a natural light-dark cycle. Methotrexate (MTX) purchased from Sigma-Aldrich (St. louis, MO, USA) administration took place one-week prior aspartame intake according to the model designed by Iyyaswamy et al., [8]. All experiments were carried with the recommendations of Suez Canal University's Institutional Animals Ethics Committee (no.5073#). The lab work took place in the Centre of Excellence in Cellular and Molecular Medicine, Faculty of Medicine, Suez Canal University.

Study design:

Male Wistar albino rats (10 animals) were used as donors for omental AD-MSCs. Adults female Wistar albino rats (40 animals) were separated into four equal groups (10 animals each) at the beginning of the experiment. The rats were subjected to standard environmental conditions and allowed free access to normal rat chow diet and water ad libitum. One week after acclimatization rats were randomly divided into three experimental groups

Group I (control group): which was subdivided into: Group I.a (saline control): the animal of which received ordinary food without any additives and received 0.5 ml saline subcutaneously. Group I.b (MTX-control group): the animal of which received MTX in sterile saline (0.2 mg /kg for a week) subcutaneously and maintained on folate-deficiency diet till the end of the study. Group II (MTX / Aspartame-treated group): rats were injected subcutaneously with MTX in sterile saline (0.2 mg /kg for a week) to cause folate deficiency which was confirmed after a week of the last MTX dose by assessment of urinary excretion of formamoinoglutamic acid (FIGLU).

Then the animals received aspartame (Sigma-Aldric, St. louis, MO, USA) orally (40 mg / kg) for 90 days, during this period the rats were maintained on folate-deficiency diet **[10]**. The selected dose of aspartame based on the human daily permitted exposure limit that was identified by the European Safety Authority (ESA) in 2006 **[11].** Group III (MTX/ Aspartame/ AD-MSCs-treated group): the rats given the same treatment protocol of group II followed by receiving a single intravenous injection of AD-MSCs ($3X10^6$ cell/ml) via the tail vein and were sacrificed 30 days after transplantation **[12].**

Folate deficient diet:

The composition of the folate deficient diet is shown in table one (Table 1). It was prepared in the animal facility of Ain Shams University's medical research centre. The diet was formed of 99% basal mix (Ain 93M, cat; TD.09171) and 1% an appropriate (folate deficient) vitamin mix (AIN 93 VX, Cat; TD94047) (both from Harlan laboratories, Inc. Madison, WI, USA) [13]. The basal mixture contained 1% succinyl sulfathiazole, which decreases folate formation by gut bacteria, making sure that the animal's diet is its sole source of folate

Isolation, culture and passaging of AD-MSCs:

The donner male animals were euthanized. Each animal's omental fat was taken out and placed in 10 ml of phosphate buffered solution (PBS) (Lonza, Belgium) including 1 percent penicillin/streptomycin (PS) (1:1) under sterile conditions. To induce enzymatic digestion and obtain the stromal vascular fraction (SVF), the omental fat was cut into tiny pieces and treated with 0.1 percent collagenase (type I) purchased from Sigma Aldrich for half hour in 37 °C with frequent pipetting. The suspension was then sieved through an 80 µm diameter disposable mesh and centrifuged for 10 mins at 1800 rpm. The cell pellet re-suspended in complete medium (CM), which contained 3.5 cm Petri dishes (5X105 cells/plate), 1 percent PS, 10 % fetal bovine serum) FBS), and 89 percent DMEM (Lonza, Belgium). Daily cell monitoring and follow-up for the primary cultured cells was conducted (P0). The first media exchange took place 48 hours after incubation, and followed exchanges happened every 3 days. The culture was trypsinized when it reached confluency (80–90%) using 0.25 percent trypsin / EDTA (Gibco, Grand Island, NY) (P1-P3). P3 cells were used for transplantation and characterization **[14]**. The lab work took place in the Centre of Excellence in Cellular and Molecular Medicine, Faculty of Medicine, Suez Canal University.

Characterization of AD-MSCs:

Using monoclonal antibodies against the hematopoietic stem cell marker (CD45) and the mesenchymal stem cell markers (CD73 and CD105), the AD-MSCs of P3 were stained immunocytochemically. The cells were fixed in the tissue culture Petri dishes after removing the CM, washing several times with PBS and fixation of the cells with cold acetone/methanol; volume to volume for 15 min.

Collection of samples, histopathological and ultrastructural examination:

After 127 days from the beginning of experiment. all animals were anaesthetised by intraperitoneal injection of 60 mg/kg ketamine and 5 mg/kg xylazine and sacrificed by cervical dislocation. The brains were obtained, divided into two groups. The first group being fixed in 10 percent neutral buffer formalin and prepared in paraffin blocks. To assess the histopathological changes, transverse sections (5 µm) were stained with Haematoxyline and Eosin (H&E) stain [15]. Paraffin sections immunohistochemically stained to identify astrocytes and apoptosis using mouse monoclonal antibodies against glial fibrillary acidic protein (GFAP) (1:200) purchased from Santa Cruz Biotechnology Inc., USA (Cat # sc-166481), and caspase-3 (1:250) purchased from R&D Systems, Minneapolis, Minn., USA (Cat# AF835-SP) [12]. The other group of the brains were carefully cut into 1cm3 piece from cortex of frontal lobe and fixed for 24 hours in (2.5 percent) buffered glutaraldehyde. They were then post-fixed (1 percent) osmium tetoxide (OSO4) in distilled water For 2 hours at 4C, dehydrated, and embedded in epoxy resin. Semi-thin sections (1 µm thick) were obtained, looked at under a light microscope, after being stained with Toluidine Blue. With the aid of an ultratome (Reichert Ultracut, Ziess, Germany), ultrathin sections 70-90 nm thickness and stained with lead citrate and uranyle acetate were cut. They were then examined and captured on camera using a transmission electron microscope (Mycotic Centre, Al-Azhar university) [16]

Morphometric analysis:

Using ImageJ (version 1.33-1.34; National Institutes of Health, Bethesda, MD, USA), the following parameters were assessed [17]:

GFAP immune-stained sections' field integrated density (IntDen). The area percent for GFAP

immunoreaction in astrocytes and their processes in frontal cortex was calculated using ten non-overlapping fields from six sections of each animal X400/sample in each group were used to measure GFAP

Average number of neurons that showed caspase-3 brownish immunoreactivity in the frontal cortex. by ten non-overlapping fields from six sections of each animal X400/sample in each group were used to measure caspase-3 immune reaction

Detection of donner male-derived AD-MSCs in female brains:

AD-MSCs were tracked in the female brains by using real time PCR assay. QIAamp® DNA Mini and Blood Mini KIT, Germany, was used to prepare the genomic DNA from the brain tissue homogenate of the rats in each group. Following the manufacturer's instructions, PCR was used to determine whether recipient female rats had the sex determination region on the Y chromosome male (sry) gene or not. Primer sequences for the sry gene were obtained from published sequences (forward: 5′-CATCGAAGGGTTAAAGTGCCA-3′, reverse: 5′-ATAGTGTGTAG-GTTGTTGTCC-3′), and an amplified product (104 bp) was purchased from (Sigma-USA) [18].

RESULTS

Primary culture and subculture of AD-MSCs results:

Examination of the isolated cells by inverted light microscope showed that: on day 3 after seeding and first exchange of media, a small population of cells appeared attached to the Petri dish substratum, the number of which increased to reach confluency by the 10th day of P0 After which subcultures were performed from P1 to P3 the cells appeared homogenous in morphology; they exhibited a fibroblast- like morphology with abundant nucleus and multiple nucleoli. They exhibited a propensity to form colonies and had interdigitating cytoplasmic processes in their granular cytoplasm (Fig. 1). Most of the attached cells showed (a positive) brownish reaction for CD 105 and CD 73 (94.5% and 91.1%, respectively) when the cultured cells on P3 were characterized using CD105, CD73, and CD 45 (Fig. 2)

Histopathological results:

Saline-Control group and MTX- control group showed the same finding regards all the study parameter so they will be referred to as control group. The frontal cortices of the control group (group I) stained with Haematoxylin and eosin showed the six different layers of the cerebral cortex (outer molecular layer - the external granular layer - external pyramidal layer - inner granular layer - inner pyramidal - polymorphic layer), they were covered with pia matter containing blood vessels (Fig. 3). The pyramidal cells represented the common neuron in the layers of the frontal cortex in addition to the granular cells and neuroglial cells. These neurons presented large vesicular nuclei, basophilic cytoplasm, and cellular processes. The granular cells showed prominent nucleoli inside their open face nuclei. The smaller neuroglia with small dark nuclei cells were dispersed in between the neuronal cells in the neuropil which also contained nerve fibres and blood vessels (Fig. 3 In Set). Frontal cortex of group II (MTX / aspartame group) appeared with vacuolated astrocyte, vacuolated neuropil, Granular cells appear with intracellular vacuolation and some of them showed pale stained nuclei. neuroglial cells appear with pale stained cytoplasm and shrunken nuclei. (Fig. 4 A). Many shrunken pyramidal cells were seen with pale-stained nuclei but some of them showed enlarged size with intracellular vacuolation (Fig. 4 B&C). Neuroglial cell infiltrate was clearly noticed in many layers of the frontal cortex (Fig. 4 B&C), Focal aggregation of many cells and condensation in the inner pyramidal & granular layer (Fig. 4 D). In the frontal cortex of AD-MSCs-treated group (group III), many of the pyramidal and the granular cells regained their normal morphology apart from some few persistent intracellular vacuolation and very few vacuolation in the neuropil. Some few granular cells showed cytoplasmic vacuolation and some appeared shrunken with condensed nucleoli and pericellular hallos. Neuroglial infiltrate and congested blood vessels had no longer noticed in this group (Fig. 5 A&B).

Immunohistochemical and morphometric results:

The immunoreactivity of GFAP: The cerebral cortex of the group I showed mild positive reaction in the astrocytes and glial fibres in all layers of the cortex; the astrocytes appeared star-shape and the fibres appear thin and regular, while in group II the immunoreactivity increased obviously (moderate positive reaction); astrogliosis and overlapping of thick processes were clearly noticed. In group III the GFAP immunoreactivity had almost regained its pattern and intensity of the control group

(moderate positive reaction) (Fig. s6). Quantification of this finding by morphometric analysis revealed a notable increase in the area percentage of GFAP in the cerebral cortex of group II (6.3 ± 0.3%, P<0.005) in comparison to the control group (0.55± 0.02%) and a significant decrease in its level in group III (1.3±0.04, P < 0.001) in comparison to group II. Between group III and the control group, there was no discernible difference (P < 0.5) (Chart s1).

The immunoreactivity of Caspase-3: very few cells of the cerebral cortices of the control group showed mild positive nuclear and cytoplasmic immunoreaction to caspase-3, on the other hand the number of caspase-3- moderately positive stained neurons increased in group II in all layers of the frontal cortex. Administration of AD-MSCs in group III decreases the expression of this marker almost to the control values (Fig. s7). These findings revealed a highly increase of the number of caspase-3 positively stained cells in group II (33.4 ± 2.3, P<0.001) in comparable to the control group (5.2 ± 0.4) and a significant decrease in their number in group III (10.2 ± 1.2, P<0.05) when compared to group II. There was no significant difference between group III and the control group (P<0.5) (Chart s2).

Transmission electron microscopic:

Transmission electron microscopy of the frontal cortex of the control group indicated normal ultrastructure of the neuron which appeared with vesicular euchromatic nucleus, prominent nucleolus, well-identified hillock and well-organized cytoplasmic organelles (normal mitochondria, rough endoplasmic reticulum (RER), and un-myelinated nerve fiber) (Fig.s8 A). The surrounding neuropil appeared normal without vacuolation and contained many nerve fibres; some of them were myelinated with a well-formed myelin sheath and many of them were non-myelinated and showed normal mitochondria (Fig. s8 A&B). The blood vessels showed no dilatation, they were lined with normal shape and size endothelium with flat nucleoli, showed erythrocytes inside, and surrounded by astrocyte foot plates which had normal size with no evidence of perivascular oedema (Fig. s8 C). The ultrastructure of the cerebral cortex of group II (MTX/aspartame-treated group) showed signs of massive neuronal degeneration, many neurons appeared with electron dense nucleus and electron dense cytoplasm which showed dilatation of the (RER). It was difficult to recognize other organelles within the cytoplasm (Fig s9 A). The surrounding neuropil showed massive vacuolations and severely degenerated nerve fibres (Fig. s9 B). The blood vessels appeared congested with erythrocytes. There was evidence of perivascular oedema in the form of abnormal astrocyte foot plates which surround the vessel. Some lining endothelium showed thickening and exhibited heterochromatic nuclei. Many glial cells mostly astrocytes appeared abnormal with hyperchromatic nucleoli and electron dense vacuolated cytoplasm (Fig. s9 D&E). Transmission electron microscopy of the frontal cortex of the group III (AD-MSCs-treated group) rats demonstrates almost restoration of the control ultrastructure of most neuron which appeared with regular euchromatic nucleus with dark prominent nucleolus and well-identified and organized cytoplasmic organelles (Fig.s10 A). The surrounding neuropil showed almost normal structure with normal blood vessels, myelinated nerve fibres (with well-formed myelin sheath), non-myelinated nerve fibres (including mitochondria with normal size and morphology), and persistent minimal vacuolation (Fig. s10 B, C). The blood vessels showed normal size with slightly dilatation of the astrocyte foot plates and myelinated, non-myelinated nerve fibres, normal glial cells euchromatic nucleus and prominent nucleolus (Fig. s10 D& E).

Detection of male AD-MSCs in female cerebral cortex:

The Y chromosome marker (Sry) gene was detected by PCR at the end of the study to be expressed in the cerebral cortex of the recipient (female) rats which were treated with male derived AD -MSCs in AD-MSCs-treated group (group III). Moreover, neither the control group nor the group that had received MTX/aspartame treatment had any signs of the Y chromosome marker (group II) (Fig. s11).

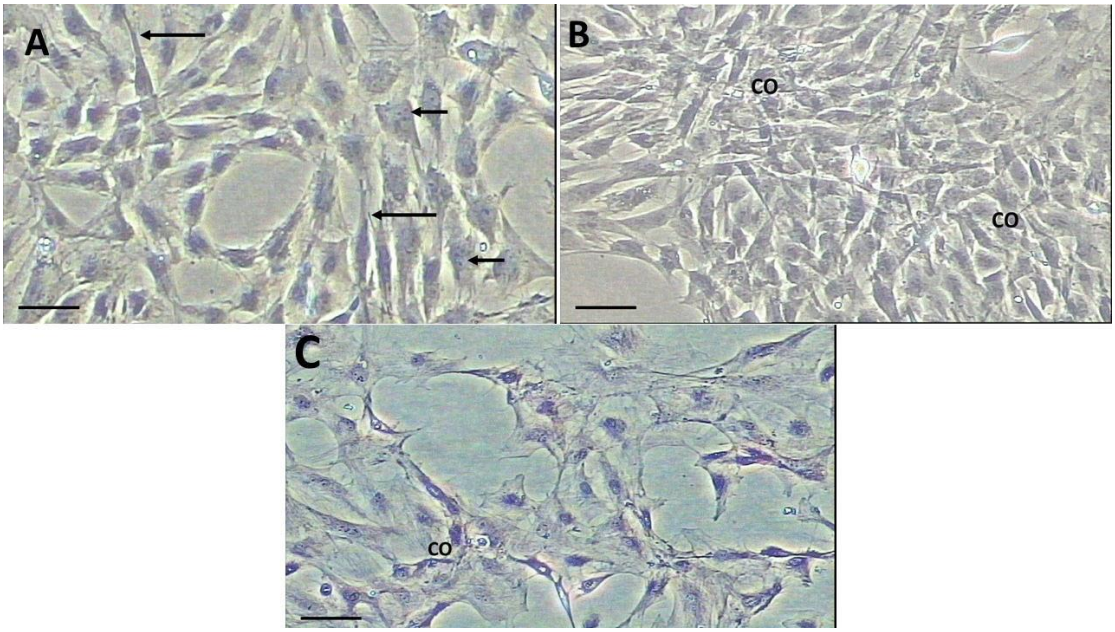

Figure 1: Photomicrographs of rat AD-MSCs. The cells appeared with abundant cytoplasm, vesicular nuclei with multiple nucleoli (short arrow) and possessed cytoplasmic processes (long arrow). The cells show about 60 % confluency a week after seeding (A) and 90% confluency at the 10th day of P0 (B). The cells showed tendency to form colonies (co) during primary culture (B) and during different passages (C). (A&B: Inverted light microscope, C: Giemsa X 200) (scale bar 50 µm)

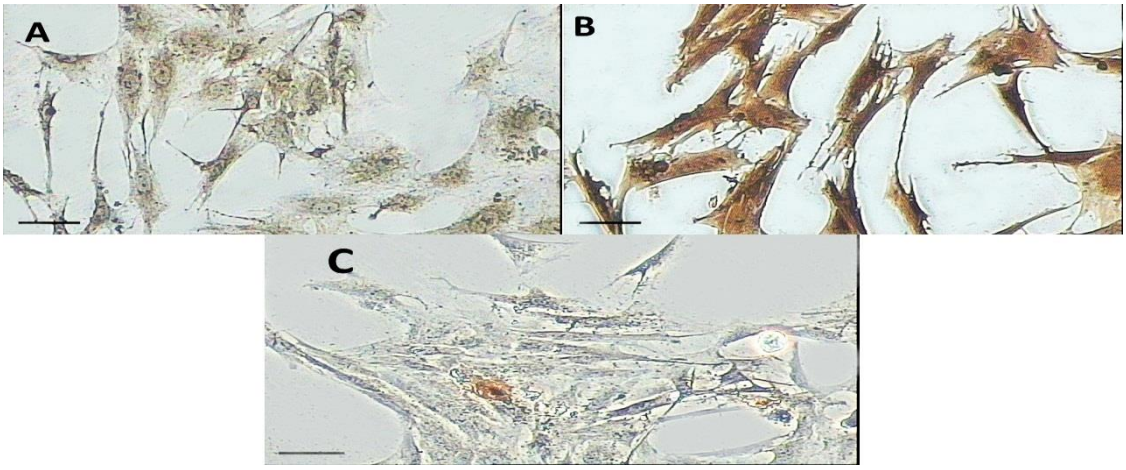

Figure 2: Photomicrographs of rat AD-MSCs. Most of the cells showed positive immunoreactivity to CD73 (A) and CD105 (B) while most of them showed negative immunoreactivity to CD 45 (C) (A&B: Inverted light microscope, C: Giemsa X 200). (scale bar 50 µm)

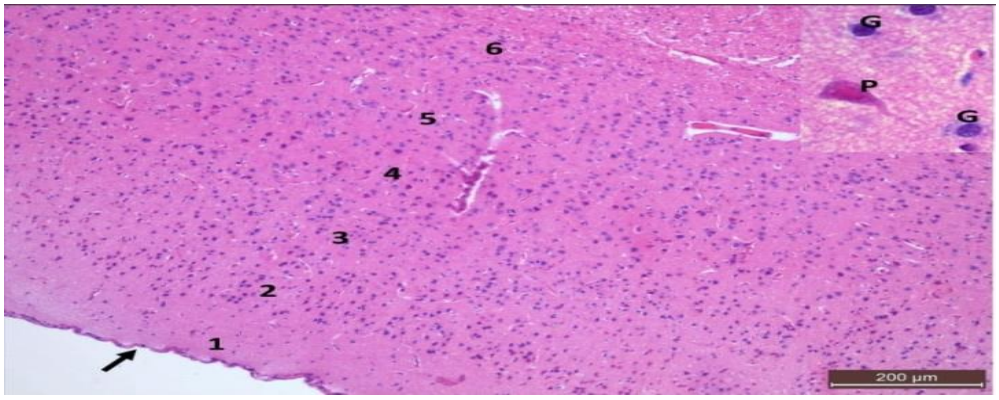

Figure 3: A photomicrograph of rat frontal cortex of the control group covered by pia matter (arrow). The different layers of the cortex are noticed; 1: the outer molecular layer, 2: external granular layer, 3: external pyramidal layer, 4: inner granular layer, 5: inner pyramidal layer and 6: polymorphic layer. (H&E X200, inset X400).

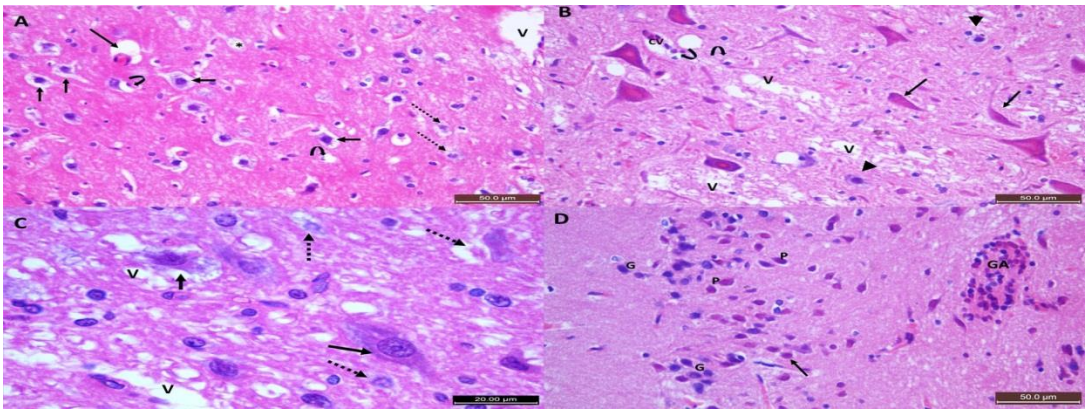

Figure 4: Photomicrographs of rat frontal cortex of group II (MTX/aspartame group) showing A): The outer granular layer showing vacuolated astrocyte (long arrow) and vacuolated neuropil (V). Granular cells appear with intracellular vacuolation (short arrow) and some of them showed pale stained nuclei (dashed arrow). neuroglial cells appear with pale stained cytoplasm and shrunken nuclei (curved arrow) (H&E X200) B): Outer pyramidal layer showing vacuolated neuropil (V), congested blood vessels (CV), shrunken nerve cells (arrow), neuroglial cell infiltrate (curved arrow) and many cells with deep stained nuclei (arrowhead)(H&E X200) C): Inner pyramidal layer showed vacuolated neuropil (V) cells with pale stained nuclei (dashed arrow), nerve cell with intracellular vacuolation (short arrow). Few normal nerve cells (long arrow) are seen X400 D) Focal aggregation of many cells in the outer pyramidal layer (GA) and condensation of pyramidal (P) and granular cells (G) in the inner pyramidal and granular layers (arrow) (H&E X200).

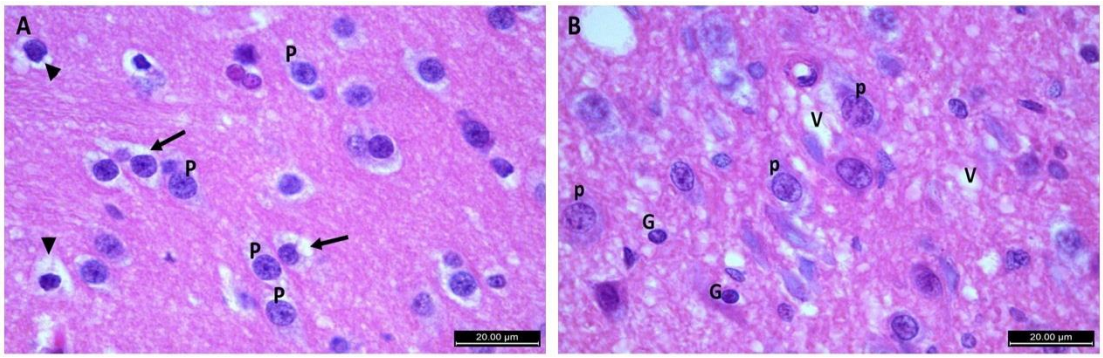

Figure 5: Photomicrographs of rat frontal cortex of group III (MTX/aspartame/ AD-MSCs group); A: outer granular layer and B: inner granular and inner pyramidal layer showing: Almost normal granular cells with open face nuclei and prominent nucleoli (G) and pyramidal cells (P) few of neuron still show cytoplasmic vacuolation (arrow) and some appeared shrunken with condensed nucleus and precellular hallo (arrow head). few persistent vacuolation (V) in the neuropil (H&E X400).

Table 1: Ingredients of folate deficient diet in different study groups.

Ingredients (g/kg)	99% basal mix	control	MTX/Aspartame & MTX / aspartame /AD-MSCs
Casein	141.41	141.41	141.41
L-cystine	1.82	1.82	1.82
Corn starch	460.29	460.29	460.29
Maltodextrin	156.5	156.5	156.5
Sucrose	101	101	101
Soybean oil	40.40	40.40	40.40
Cellulose	50.51	50.51	50.51
Ain-93M, mineral mix	35.35	35.35	35.35
Choline bitartrate	2.53	2.53	2.53
TBHQ antioxidant	0.01	0.01	0.01
Succinyl sulfathiazole	10.10	10.10	10.10
Folate sufficient vitamin mix	---------	10	--------
Folate deficient vitamin mix	--------	----------	10

DISCUSSION

Aspartame, sucralose, saccharin, acesulfame-K, and neotame are five commonly used artificial sweeteners that have received FDA approval. Apart from the herbal extract, stevia, and the sugary alcohol erythritol, which have limited applications, [16]. Among these sweeteners, over 90 countries and 6,000 products use aspartame more frequently than any other synthetic non-nutritive sweetener. [17]. Several recent large and long-term studies in rats have demonstrated its adverse effects on the brain. [18]. It was also implicated in many neurodegenerative illnesses such as Alzheimer and parkinsonism [19] in the current study the efficacy of AD-MSCs to restore the structure and ultrastructure of the rat cerebral cortex after long-term aspartame intake was evaluated. The current study's histopathological findings revealed numerous morphological and pathological changes in the rat frontal cortex, including almost all pyramidal cells, microglia, and granular cells. Focal aggregation was also noticed in the external pyramidal layer and the neuropil appeared vacuolated, after daily usage of aspartame (40 mg/kg) for 90 days. These findings corroborate previous research that found inflammation, vacuolation, necrosis, gliosis, and apoptosis as pathological changes in the cerebral cortices after aspartame consumption [1, 19].

The current work's histopathological findings were in concomitant with significant increases in caspase-3 and GFAP expression in the cerebral cortex, indicating that aspartame has a degenerative and apoptotic effect. Consuming aspartame over an extended period may lead to the production of a variety of free radical species,

including nitrogen and oxygen species. These free radicals have been proven to harm DNA and proteins in cells, and they can also harm membranes by peroxiding unsaturated fatty acids in phospholipids found in cell membranes, altering their structural and functional properties. It was also established that the toxic effect of aspartame on brain tissue, as well as the release of free radicals, causes apoptosis and the release of the apoptotic marker. -3 Caspase [1, 20].

Bondy, 1989 [21], also explained aspartame's neurotoxic effect by activating calcium channels in the cell membrane via stimulation of specific receptors, resulting in calcium influx inside the neuron and subsequent activation of a cascade of events that resulted in free radical release and lipid peroxidation, both of which damage the cell. Aspartame is also considered an excitotoxin because the influx of calcium excites the neurons, causing it to discharge impulses indefinitely until death. Aspartame was also claimed to act as a chemical stressor by raising plasma cortisol levels and promoting the production of an excessive amount of free radicals. High levels of cortisol and too many free radicals may make the brain more vulnerable to oxidative stress, which could harm neurobehavioral health [22].

GFAP, a cytoplasmic filament protein, is present in astrocytes and is up regulated in response to CNS injury induced hypertrophy and hyperplasia [23]. The degree of injury was directly related to the intensity of GFAP expression. The reactive gliosis is a response to all types of CNS insults and can be mild or severe; the former is a pro-reparative phenotype in which astrocyte activation occurs, resulting in the secretion of the cytokine interleukin 1 (IL-1), which promotes neuronal survival. [24] The latter is an inhibitory phenotype in which astrocytes are in a highly reactive state, secreting cytokines such as TNF-, which has been shown in vitro to cause oligodendrocyte and myelin damage. As a result, GFAP has emerged as an ideal marker for the immunohistochemical identification of astrocytes. [25] Its reactivity is widely recognized as a sensitive and reliable marker for neurological insults [26, 27]. In the current study, group II exhibited astrogliosis, additionally a significant rise in the area percentage of astrocyte immunoreaction expression (GFAP expression). This was similar to Onaolapo et al., 2017 [28], as they stated that in chronic administration of mice caused cerebral oxidative stress, histopathological changes, and GFAP-reactivity in the cerebral cortex, as well as behavioral changes.

The ultrastructure abnormalities detected in the MTX/aspartame group confirm the degenerative and apoptotic effect of aspartame as many neurons and neuronal cytoplasmic organelles appeared degenerated, REC exhibited dilatation and many nuclei were obviously shrunken with heterochromatin. Abnormality of astrocyte foot plates and vacuolated neuropil was also evident in the current research. The altered ultrastructure is similar to the findings of Omar [1] who proved that four weeks of cessation of aspartame was insufficient to achieve a normal histological appearance of the rat frontal cortex after receiving it orally in a dose of (250 mg/kg/day) for eight weeks. The intensity of the neurodegenerative changes reported in the MTX/aspartame-treated group in the current study were obviously diminished in the MTX/aspartame AD-MSCs-treated group (group III), most of the pyramidal and the granular cells regained their normal morphology a part from some persistent intracellular vacuolation and very few vacuolations in the neutrophil. This is consistent with the findings of numerous researchers [29, 30]. In comparison to the MTX/Aspartame treated group, the area percentage of astrocytes (GFAP immunohistochemical expression) and the number of caspase-3 immune-reactive cells decreased significantly. The cerebral cortices of group III almost exhibited the control morphology regarding their ultrastructure, evidenced by the restoration of the neuronal ultrastructure and the well-myelinated nerve fibers. These findings reflect the reparative power of AD-MSCs. Mothe and Tator [31] proved that adult neural stem cells have the capability to change into either oligodendrocytes or Schwann-like cells (depending on the host environment). Both types of cells can myelinate axons in the demyelinated or dysmyelinated adult spinal cord.

Due to their multipotency AD-SCs are well suited for a variety of therapies in regenerative medicine. Adipose tissue, as opposed to bone marrow, is a rich source of stem cells that are simple to isolate in sufficient quantities with little morbidity. Furthermore, the immunosuppressive characteristics of AD-SCs make them a desirable and clinically significant cell population for cytotherapy [1]. Many studies have shown that MSCs protect the damaged CNS and fix it in different ways. For example, they could help native neural stem cells grow, move, and change by releasing chemokines or indirectly by

activating the astrocytes in the area. [32]. In addition to their role in axon myelination, activated astrocytes enhance neuronal survival by providing cholesterol and energy to neurons, as well as assisting in the survival, proliferation, and maturation of oligodendrocyte precursor cells. [33]. It has also been shown that activated astrocytes control the transmission of synaptic signals and change synapses by removing excitotoxic molecules from the extracellular space, which helps neurons live longer. [34]. The ability of MSCs to change into cells that act like neurons and glia was used to explain another mechanism. [35].

The ameliorating effects of MSCs on rat brain was also proved by Donega et al., [36]. They thought that MSCs pushed microglia toward the M2 phenotype, which helps repair tissue in addition to reducing inflammation. After 15 days of MSC transplantation in mice with an ischemic brain injury, they saw a decrease in the number of GFAP+ cells, which shows that MSCs can reduce gliosis. Another study showed the paracrine effect of stem cells and their ability to secrete bioactive molecules like anti-inflammatory cytokines, trophic and growth factors, interleukin IL-6, IL-7, IL-8, IL-11, IL-15, macrophage colony-stimulating factor, and stem-cell factor. These molecules are what give stem cells their anti-inflammatory and anti-apoptotic properties. [32]. MSCs taken from the vascular stromal fraction of adipose tissue and the umbilical cord release trophic/neuroregulatory factors that make cultured hippocampal neurons more metabolically viable and increase the number of neuronal cells [37]. Stem cell therapy in brain injury was mistakenly limited due to the belief that they are unable to cross the BBB; however, recent research demonstrated their ability to cross the BBB by their affinity to become adherent to the injured tissue endothelium by certain adhesion molecules; VCAM-1/VLA-4 and their invasion and recruitment to the recipient tissue using plasmic podia. [38]. Homing of AD-MSCs into the rat cerebral cortex was evident in the current work by detection of the Y chromosome marker; (Sry) gene by PCR in the cerebral cortices of the recipient female rats.

CONCLUSIONS

Chronic aspartame consumption leads to detectable histopathological and ultrastructural alteration of rat cerebral cortex reflecting its apoptotic and degenerative effect. This alteration was greatly ameliorated by AD-MSCs transplantation which was traced into the recipient rat cerebral cortices and proved to decrease gliosis and apoptosis in such tissue.

RECOMMENDATIONS

There is still much to learn about mesenchymal stem cells (MSCs) to consider a novel source for cytotherapy and regenerative medicine. More research is needed to find out how the transplanted cells in brain tissue will act and live in the long run.

Conflict(s) of interest: None
Financial Disclosures: None

REFERENCES

1. **Omar SMM.** Effect of aspartame on the frontal cortex of adult male albino rats. A light and electron microscopic study. Egypt. J. Histol. 2009; 32(2):346–357.
2. **Karol R, Jadwiga Elżbieta JA.** Effects of aspartame metabolites on astrocytes and neurons. Folia Neuropatholgica. 2013; 51 (1): 10-17.
3. **Gombos K, Varjas T, Orsós Z et al.** The effect of aspartame administration on oncogene and suppressor gene expressions. In Vivo 2007;21: 89–92.
4. **Iyyaswamy A, Rathinasamy S.** Effect of chronic exposure to aspartame on oxidative stress in the brain of albino rats. J. Biosci. 2012; 37(679-688).
5. **Mourad I M, Noor NA.** Aspartame (a widely used artificial sweetener) and oxidative stress in the rat cerebral cortex. Int J Pharm Biomed Sci 2011; 2 (1), 4-10.
6. **Iyyaswamy A, Rathinasamy S.** Biochemical responses and mitochondrial mediated activation of apoptosis on long-term effect of aspartame in rat brain. Redox Biology. 2014; 2 (820–831).
7. **Humphries P, Pretorius E., Naude H.** Direct and indirect cellular effects of aspartame on the brain. European Journal of Clinical Nutrition 2008; 62, 451–462.
8. **Iyyaswamy A, Rathinasamy S, Dapkupar W.** Acute effect of aspartame-induced oxidative stress in Wistar albino rat brain. Journal of Biomedical Research. 2015; 29 (5):390-396.
9. **Leu S, Lin YC, Yuen CM, Yen CH et al.** Adipose-derived mesenchymal stem cells markedly attenuate brain infarct size and improve neurological function in rats. J Transl Med. 2010. Jun 28; 8:63.

10. **Mattes RD, Popkin BM.** Nonnutritive sweetener consumption in humans: effects on appetite and food intake and their putative mechanisms. Am J Clin Nutr. 2009; 89:1-14
11. **Crivello NA, Blusztajn JK, Smith DE.** Short-term nutritional folate deficiency in rats has a greater effect on choline and acetylcholine metabolism in the peripheral nervous system than in the brain, and this effect escalates with age. Nut Res. 2010; 30(10)722-730). doi: 10.1016/j.nutres. 2010.09.008.
12. **Palumbo P, Lombardi F, Siragusa G et al.** Methods of Isolation, Characterization and Expansion of Human Adipose-Derived Stem Cells (ASCs): An Overview. Int J Mol Sci. 2018; 19(7): 189.
13. **Galhom RA, Abd El Raouf HHH, Ali MHA.** Role of bone marrow derived mesenchymal stromal cells and Schwann-like cells transplantation on spinal cord injury in adult male albino rats. Biomed. Pharmacother. 2018; 108, 1365–1375.
14. **Abdel khalek, H A, Fikry H. Sara AS.** Protective effect of bone marrow-derived mesenchymal stem cells on methotrexate-induced brain and liver injury in female albino rats: Histological study. Stem Cell 2017; 8 (1).
15. **Liu X, Liao X, Luo E et al.** Mesenchymal stem cells systemically injected into femoral marrow of dogs home to mandibular defects to enhance new bone formation, Tissue Eng. 2014; Part A. 20(3-4): 883–892.
16. **Akhalq AF.** Effect of soft drinks consumption in human In "High calorie diet and human brain: metabolic consequence of long term consumption". Chapter 5 P:140-144. Springer International Publishing Switzerland, 2015.
17. **Tandel KR** Sugar substitutes: health controversy over perceived benefits. J. Pharmacol Pharmacother 2011; 2:236–243.
18. **Ashok l, Sheeladevi R, Wankhar D.** Long term effect of aspartame (artificial sweetener) on membrane homeostatic imbalance and histopathology in the rat brain. Free Rad Antioxidants. 2013; 3: S42–9. 5.
19. **Okasha EF.** Effect of long term-administration of aspartame on the ultrastructure of sciatic nerve. J Microsc Ultrastruct. 2016; 4(4): 175–183.
20. **Abhilash M, Paul MVS, Arghese MVV, Nair RH.** Effect of long term intake of aspartame on antioxidant defense status in liver. Food Chem Toxicol. 2011; 49: 1203–7.
21. **Bondy SC.** Intracellular calcium and neurotoxic events. Neurotoxicol Teratol. 1989; 11(6):527-31. doi: 10.1016/0892-0362(89)90032-9.
22. **Choudhary AK, Lee YY.** Neurophysiological symptoms and aspartame: What is the connection? Nutr Neurosci. 2018; 21(5):306-316. doi: 10.1080/1028415X.2017.1288340
23. **Abou-Donia MB, Khan WA, Suliman HB et al.** Stress and combined exposure to low doses of pyridostigmine bromide, DEET, and ermethrin produce neurochemical and neuropathological alterations in cerebral cortex, hippocampus, and cerebellum. J Toxicol Environ Health. 2004; 67:163–192.
24. **Choi SS, Lee HJ, Lim I et al.** Human Astrocytes: Secretome Profiles of Cytokines and Chemokines. PLoS ONE (2014);9(4): e92325. https://doi.org/10.1371/journal.pone.0092325
25. **Sofroniew MV, Vinters HV** Astrocytes: biology and pathology. Acta Neuropathol. 2010; 119:7–35.
26. **Axelsson M, Malmeström C, Nilsson S et al.** Glial fibrillary acidic protein: a potential biomarker for progression in multiple sclerosis.J of Neurolo. 2011;258(5),882-888.
27. **Yang Z, Wang KK.** Glial Fibrillary acidic protein: From intermediate filament assembly and gliosis to neurobiomarke. Trends in Neurosci. 2015; 38(6), 364–374.
28. **Onaolapo AY, Onaolapo OJ, Nwoha PU.** Aspartame and the hippocampus: Revealing a bi-directional, dose/time-dependent behavioural and morphological shift in mice. Neurobiol. Learn. Mem. 2017;139,76.
29. **Liu PK.** Ischemia reperfusion-related repair deficit after oxidative stress: implications of faulty transcripts in neuronal sensitivity after brain injury. J Biomed Sci. 2003; 10: 4e13.
30. **Frese L, Dijkman PE, Hoerstrup SP.** Adipose Tissue-Derived Stem Cells in Regenerative Medicine. Transfus Med Hemother. 2016; 43:268–274.
31. **Mothe AJ, Tator CH.** Transplanted neural stem/progenitor cells generate myelinating oligodendrocytes and Schwann cells in spinal cord demyelination and dysmyelination. Exp Neurol. 2008; Sep;213(1):176-90. doi:

10.1016/j.expneurol.2008.05.024. Epub 2008 Jun 10.

32. **Meirelles S, Fontes M, Covas T et al.** Mechanisms involved in the therapeutic properties of mesenchymal stem cells. Cytokine Growth Factor Rev. 2009, 20:419-427.
33. **Hülya K, Susan LL, Hosseinzadeh S et al.** The multifaceted role of astrocytes in regulating myelination. Experimental Neurology. 2016; 283, (B), 541-549.
34. **Krum JM, Philips TM, Rosenstein JM.** Changes in astroglial GLT-1 expression after neural transplantation of stab wound. Exp. Neurol. 2002; 174,137-149.
35. **Sharma A, Sane H, Kulkarni P et al.** Cell therapy attempted as a novel approach for chronic traumatic brain injury. a pilot study. Springer Plus 2015; 4:26.
36. **Donega V, Nijboer CH, Tilborg GV, et al.** Intranasally administered mesenchymal stem cells promote a regenerative niche for repair of neonatal ischemic brain injury. Experimental Neurology. 2014; 261: 53–64.
37. **Ribeiro CA, Fraga JS, Grãos M et al.** The secretome of stem cells isolated from the adipose tissue and Wharton jelly acts differently on central nervous system derived cell populations. Stem Cell Res Ther 2012; 3:18.
38. **Steingen C, Brenig F, Baumgartner L et al.** Characterization of key mechanisms in transmigration and invasion mesenchymal stem cells. J Mol Cell Cardiol. 2008; 44:1072–1084.

To Cite :

Almallah, A., galhom, R., kamel, E. Role of Adipose-derived stem cells in restoration of histological structure of rat frontal cortex after chronic aspartame intake. *Zagazig University Medical Journal*, 2024; (95-111): -. doi: 10.21608/zumj.2022.172531.2673.

Supplementary file

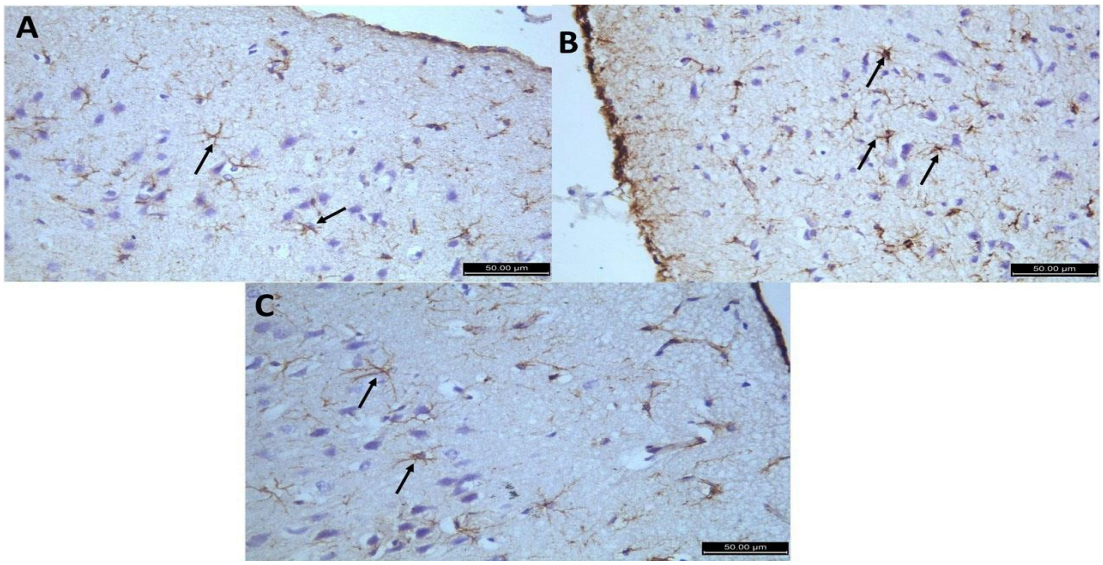

Figure 6: Photomicrographs of rat cerebral frontal cortices of all groups, astrocytes GFAP immunoexpression in granular layer (arrows) is mild in control rats (A); while moderate in group II (MTX/Aspartame-treated group) with thick processes (B); positively mild stained astrocytes with fine processes are seen in AD-MSCs-treated group (group III) (C) (anti-GFAP X400).

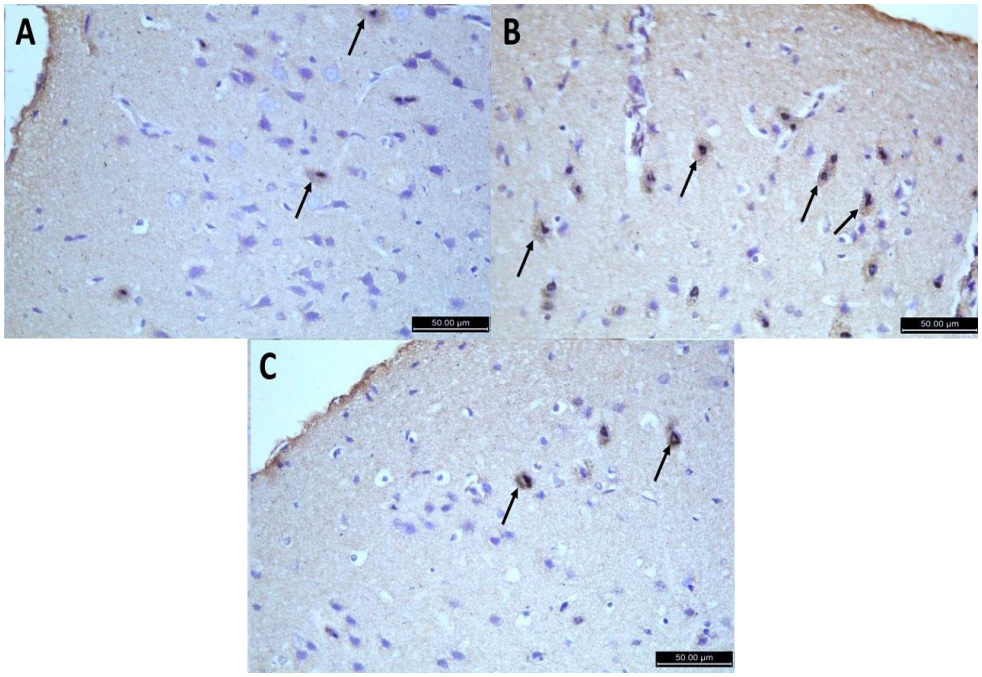

Figure 7: Photomicrographs of rat cerebral cortices of all groups, immunohistochemically stained with anti- caspase-3 monoclonal antibody showing mild nuclear and cytoplasmic positive brown reaction in few cells of the frontal cortex of the control group (A) and AD-MSCs-treated group (group III) (C) while in group II (MTX/Aspartame-treated group) (B) are moderately-stained. (Anti-caspase-3 X400).

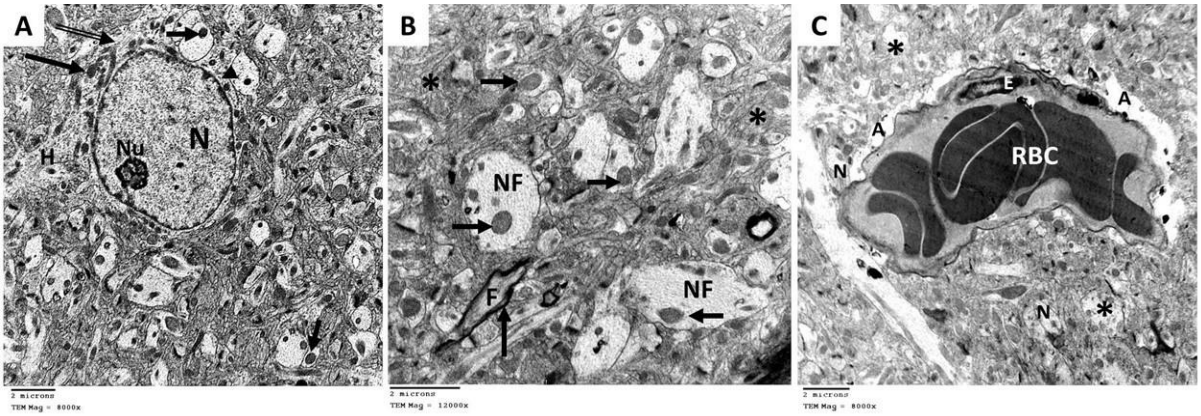

Figure 8: Transmission electron microscopy of the frontal cortex of the control rats showing: A) normal neuron with euchromatic nucleus (N) and a dark prominent nucleolus (Nu). The cell has a well-recognized hillock (H), normal mitochondria (long arrow), rough endoplasmic reticulum (double arrow) and unmyelinated nerve fibre(arrowhead). The neuropil around the neuron had many non-myelinated nerve fibres with normal mitochondria (short arrow). B) normal neuropil (asterisks) with myelinated nerve fibres (F) with well-formed myelin sheath (long arrow) and non-myelinated nerve fibres (NF) with normal mitochondria (short arrow). C) neuropil (asterisks) containing many nerve fibres (N) and a blood vessel lined with normal endothelium (E) with flat nucleus and contains red blood cells (RBC). The vessel is surrounded by normal shaped and sized astrocyte foot plates (A). Original magnification A: X8000, B: X12000, C: X800

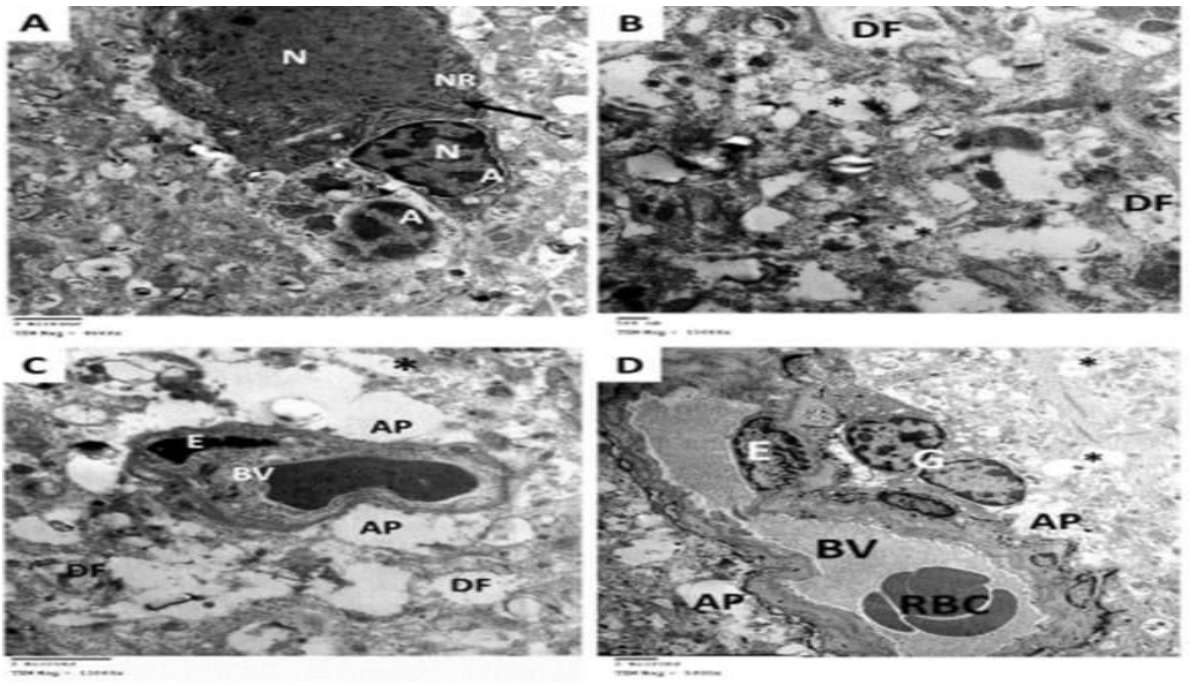

Figure 9: Transmission electron microscopy of the frontal cortex of group II (MTX/aspartame-treated group) rats showing: A) degenerated dark neuron (NR) containing electron dense nucleus (N) and electron dense cytoplasm with dilated rough endoplasmic reticulum (long arrow). Abnormal astrocytes (A) are noticed with heterochromatic nuclei (N), disintegrated cytoplasmic organelles and vacuolation. B): massively vacuolated neuropil (asterisks) with multiple degenerated nerve fibres (DF). (C &D): Blood vessels (BV) containing red blood cells (RBC) and are lined with thickened endothelium (E) and surrounded by abnormal astrocyte foot plates (AP). Notice the two glial cells (G) with heterochromatic

nucleoli and electron dense vacuolated cytoplasm, Original magnification A: X8000, B: X15000, C: X12000, D: X5000

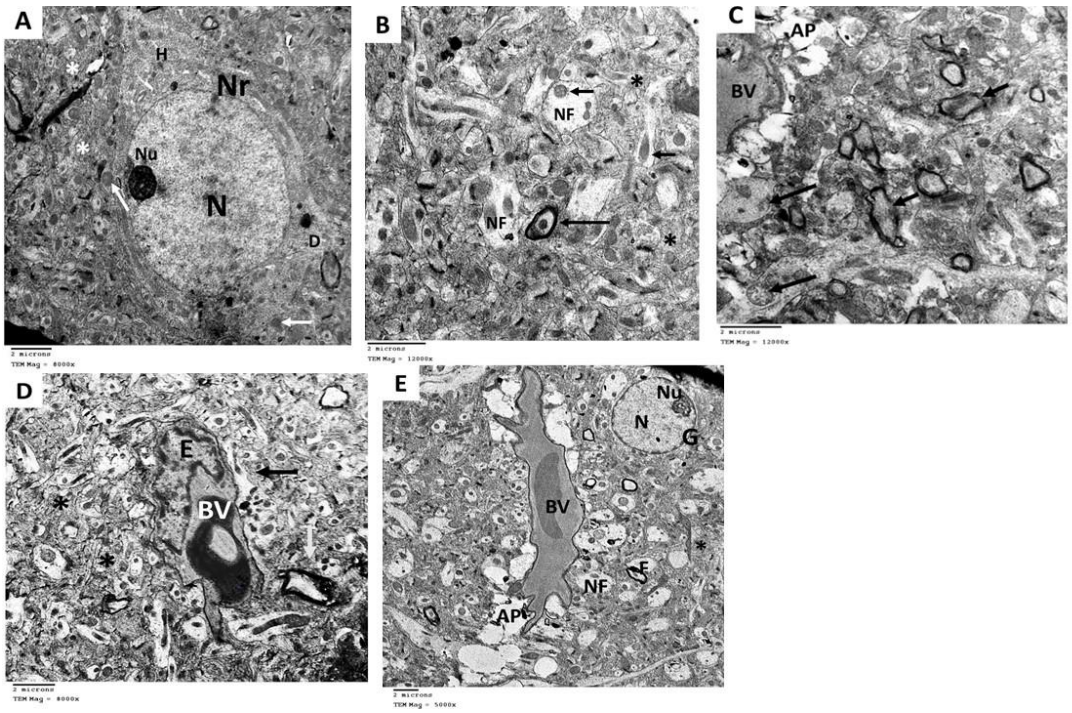

Figure 10: Transmission electron microscopy of the frontal cortex of the group III (AD-MSCs-treated group) rats showing: A) normal neuron (Nr) with euchromatic nucleus (N) and a dark prominent nucleolus (Nu). The cell has a well-recognized hillock (H), dendrite (D), normal mitochondria (white arrow). B) neuropil (asterisks) containing myelinated (long arrow) and non-myelinated (NF) nerve fibres with normal mitochondria (short arrow). C): Apparent normal astrocyte foot plate (AP) around blood vessels (BV). The surrounding neuropil contained nonmyelinated nerve fibre (long arrow) and normally myelinated nerve fibres (short arrow)X12000 D): Blood vessels (BV) still showing thickening in the lining endothelium (E); the nucleus of which appeared heterochromatic F): minimally vacuolated neuropil containing normal blood vessels (BV) with slightly dilated astrocyte foot plate (AP), myelinated (F), non-myelinated (NF) nerve fibres and normal glial cells (G) with euchromatic nucleus (N), prominent nucleolus (Nu) Original magnification A:X8000, B: X12000, D:X512000, E:X8000.

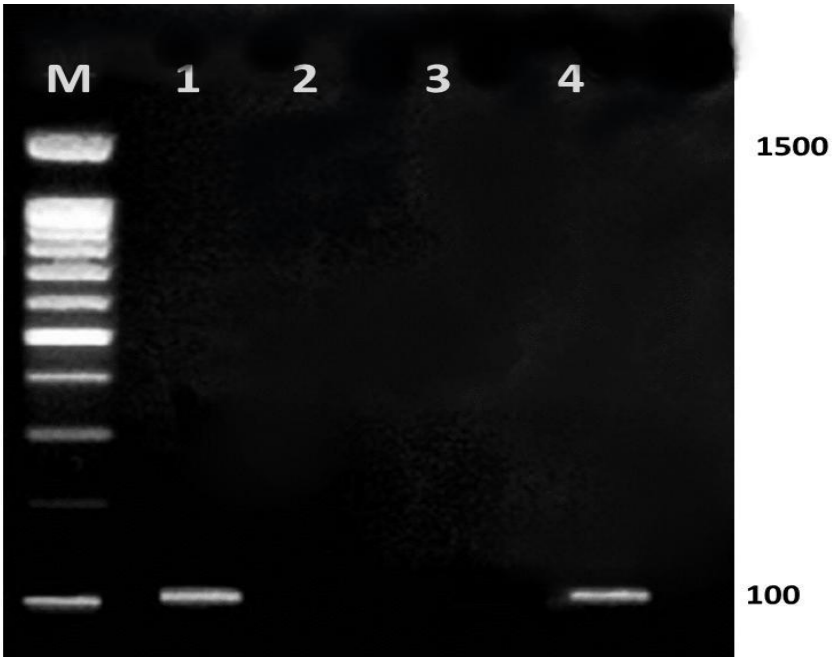

Figure 11: Agarose gel electrophoresis of *Sry* gene PCR products in different studied groups: showing detection of Y chromosome in the AD-MSCs donor male rats (lane 1) and the recipient female rats treated with male AD-MSCs in group III (lane 4). Y chromosome marker is not detected in control female rats (lane 2) and in female rats of group II (lane 3). M: PCR marker (U.V.trans-illumination).

Chart 1

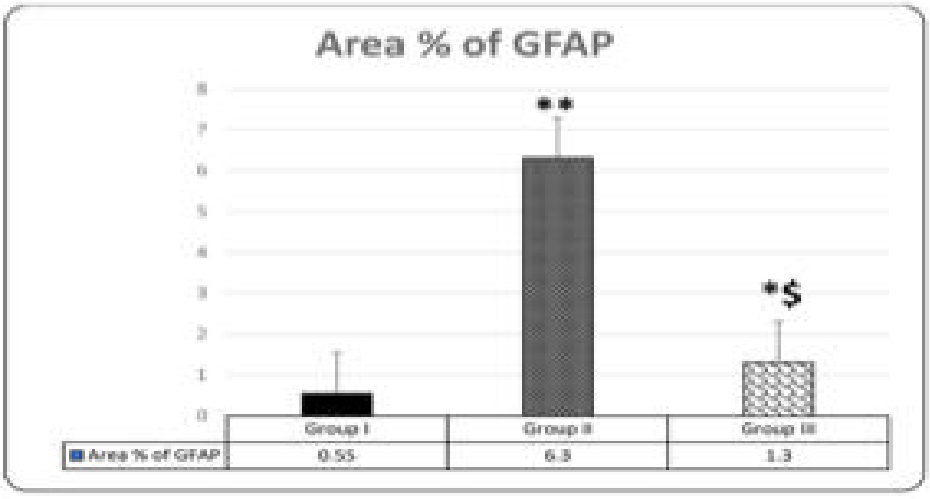

Chart 1: A chart showing Mean ± SD of area % of positive GFAP immune reaction in rat cerebral cortex of all groups

*: P< 0.5 when compared to the control group (group I)

**: P< 0.005 when compared to the control group (group I)

$: P< 0.001 when compared to group I

Chart 2

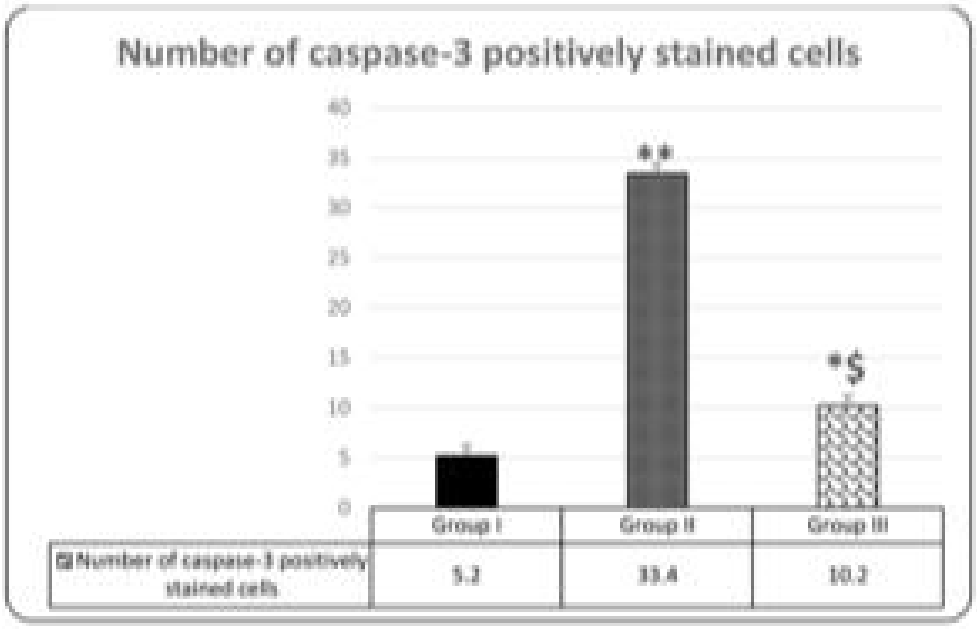

Chart 2: A chart showing Mean ± SD of the number of caspase-3 + ve immuno-reactive cells/HPFs in the rat cerebral cortex in all groups

*: P< 0.5 when compared to the control group (group I)

**: P< 0.001 when compared to the control group (group I)

$: P< 0.05 when compared to group II